Eur. Phys. J. Special Topics **223**, 2177–2188 (2014)

DOI: 10.1140/epjst/e2014-02257-0

THE EUROPEAN PHYSICAL JOURNAL SPECIAL TOPICS

Review

Relativistic lattice kinetic theory: Recent developments and future prospects

S. Succi[3], M. Mendoza[2], F. Mohseni[2], and I. Karlin[1]

[1] ETH Zürich, Department of Mechanical and Process Engineering, Sonneggstrasse 3, ML K 20, 8092 Zürich, Switzerland
[2] ETH Zürich, Computational Physics for Engineering Materials, Institute for Building Materials, Wolfgang-Pauli-Strasse 27, HIT, 8093 Zürich, Switzerland
[3] Istituto per le Applicazioni del Calcolo C.N.R., via dei Taurini 19, 00185 Rome, Italy

Received 27 April 2014 / Received in final form 18 August 2014
Published online 24 October 2014

Abstract. In this paper, we review recent progress in relativistic lattice kinetic theory and its applications to relativistic hydrodynamics. Two methods for constructing the discretised distribution function, moment matching and projection onto orthogonal polynomials, are described. Extensions to ultra-high velocities as well as improved dissipation models are discussed. We show that the existing models can successfully cover a wide range of velocities (from weak-relativistic to ultra-relativistic) and viscous regimes. Various applications, from quark-gluon plasma and relativistic Richtmyer-Meshkov instability to flows in curved manifolds are also explored. Finally, potential developments for general relativity are outlined along with future prospects for solving the full set of Einstein equations of general relativity.

1 Introduction

Lattice kinetic theory [1–3] has evidenced a major boost of activity in the last two decades, with major applications in the simulation of complex flows, from turbulence to transport in porous media and many others [4–6]. The vast majority of such applications deals with classical (non-quantum) non-relativistic fluids. However, recently, relativistic versions of the lattice Boltzmann (RLB) equation have been formulated, and applied to a number of relativistic fluid dynamic problems, such as shock waves in quark-gluon plasmas and electronic flows in graphene.

In fact, relativistic fluid dynamics plays an important role in many fields of modern physics, from large-scale applications in astrophysics and cosmology, to microscale electron flows in graphene [7–10], all the way down to quark-gluon plasmas [11,12]. The dynamics of such systems requires solution of highly nonlinear equations, making the analytic treatment of practical problems extremely difficult. Hence, various numerical methods have been developed to study the relativistic hydrodynamics. However, most of these methods are focused on the solution of the corresponding relativistic macroscopic conservation equations [13,14].

Relativistic lattice Boltzmann fills out a missing entry in the remarkably broad spectrum of LB applications across most areas of fluid dynamics [15]. Recent works have shown that the relativistic LB (RLB) stands concrete chances of carrying the well known advantages of LB schemes for classical fluids, over to the relativistic context. Among others, we refer to mathematical simplicity/computational efficiency, especially on parallel computers, and easy handling of complex geometries. In this paper, we review the main ideas behind the RLB method and outline prospective developments for future applications in cosmology and general relativistic flows.

2 Relativistic lattice kinetic theory

The relativistic Boltzmann equation, based on the Marle collision operator [16], reads as follows:

$$p^\mu \partial_\mu f = -\frac{m}{\tau}(f - f^{\mathrm{eq}}), \tag{1}$$

where f is the probability distribution function, τ the relaxation time and m is the particle mass. In the above, f^{eq} is the Maxwell-Jüttner equilibrium distribution, which reads as follows:

$$f^{\mathrm{eq}} = A \exp(-p_\mu U^\mu / k_B T). \tag{2}$$

Here, A is a normalisation constant, k_B the Boltzmann constant, T the temperature, and $(p^\mu) \equiv (E/c, \boldsymbol{p})$ the 4-momentum, with c the speed of light. The energy of the particles with mass m is defined by $E \equiv cp^0 = mc^2/\sqrt{1 - v^2/c^2}$, and the three-dimensional momentum vector $\mathbf{p} = m\mathbf{v}/\sqrt{1 - v^2/c^2}$. The macroscopic 4-velocity is given by $(U^\mu) = (c, \mathbf{u})\gamma(u)$, with $\mathbf{u}$ the three-dimensional velocity, and $\gamma(u) = 1/\sqrt{1 - u^2/c^2}$ the Lorentz's factor.

A more general single relaxation time model for relativistic Boltzmann equation was proposed by Anderson and Witting [17],

$$p^\alpha \partial_\alpha f = -\frac{U_\alpha p^\alpha}{\tau c^2}(f - f^{\mathrm{eq}}), \tag{3}$$

which gives a more accurate approximation of the transport coefficients at high temperatures, the so-called ultra-relativistic regime. Both models reproduce, at the macroscopic level, the conservation equations, i.e. $\partial_\mu T^{\mu\nu} = 0$ and $\partial_\mu N^\mu = 0$, where $T^{\mu\nu} = (\epsilon + p)U^\mu U^\nu - p\eta^{\mu\nu} + \pi^{\mu\nu}$ and $N^\mu = nU^\mu$. Here, $T^{\mu\nu}$ denotes the energy-momentum tensor, N^μ the four-particle flow, $\eta^{\alpha\beta}$ the Minkowski metric tensor (in this paper, the signature $(+,-,-,-)$ is used), ϵ the energy density, p the hydrostatic pressure, n the particle number density, and $\pi^{\mu\nu}$ is the dissipation tensor. In the following, we will briefly describe several RLB models based on relativistic kinetic theory.

2.1 Moment matching

In this section, the RLB scheme based on the moment-matching procedure is described. The moment-matching procedure means that the local kinetic equilibrium is expressed as polynomial in the relativistic fluid velocity $\beta = |\mathbf{u}|/c$, with the coefficients fixed by the condition of matching the analytic expression of the relevant relativistic moments, namely the number density and energy-momentum. The first RLB was proposed by using two distribution functions, f_i and g_i, and two Boltzmann

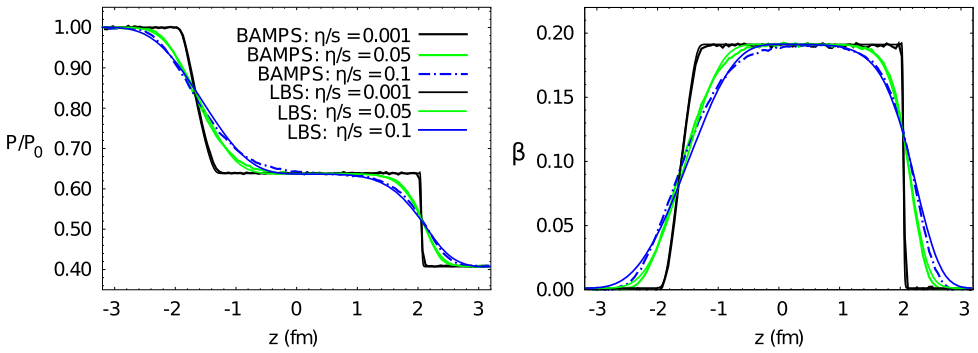

Fig. 1. Comparison between BAMPS simulations [19] and lattice Boltzmann results at t=3.2fm/c. Pressure (left) and velocity (right) of the fluid as function of the spatial coordinate z.

equations, one for the conservation of the number of particles, and one for the conservation of the energy and momentum. The discretized Boltzmann equation based on Marle collision operator takes the form ($m = 1$)

$$f_i(\mathbf{x} + \mathbf{c_i}\delta t, t + \delta t) - f_i(\mathbf{x}, t) = -\frac{\delta t}{\tau}(f_i - f_i^{\mathrm{eq}}), \tag{4}$$

where $\mathbf{c_i}$ are the microscopic lattice velocities. A companion equation holds for g_i.

We write the equilibrium lattice distribution functions as [18],

$$f_i^{\mathrm{eq}} = w_i[A + \mathbf{c}_i \cdot \mathbf{B}], \quad i \geqslant 0, \tag{5a}$$

$$g_i^{\mathrm{eq}} = w_i[C + \mathbf{c}_i \cdot \mathbf{D} + \mathbf{E} : (\mathbf{c_i c_i} - \alpha \mathbf{I})], \quad i > 0, \quad g_0^{\mathrm{eq}} = w_0[F], \tag{5b}$$

where α, A, $\mathbf{B}$, C, $\mathbf{D}$, $\mathbf{E}$, and F are coefficients to be fixed by matching the discrete macroscopic moments with their continuum versions. A lattice with the D3Q19 (19 speeds in 3 spatial dimensions) cell configuration is used. Performing a Chapman-Enskog expansion, it can be shown that the LB equations reproduce the continuum fluid equations.

To test the model, we solve the Riemann problem in viscous quark-gluon plasma [19] with an ultra-relativistic equation of state ϵ=3P. Figure 1 shows the results for different values of η/s (η is the shear viscosity and s is the entropy density) and the comparison with the microscopic transport model BAMPS [19], for low relativistic regime ($\beta \sim 0.2$). Here we can appreciate a very good agreement for different values of η/s.

For quark-gluon plasma simulations, the present lattice-kinetic algorithm appears to be nearly an order of magnitude faster than corresponding hydrodynamic codes. This is due to the fact that, at variance with any hydrodynamic representation, LB moves information along constant light-cones rather than space-time changing material fluid streamlines, which is a major simplification of the Riemann problem. For more information see Ref. [18].

2.2 Projection onto orthogonal polynomials and extension to high velocities

The moment-matching procedure described in Sect. 2.1 does not provide a unique solution for the discrete equilibrium distribution function. Here, analogous to the classical procedure of expanding the Maxwell-Boltzmann distribution in Hermite polynomials, we develop a RLB model by expanding the Maxwell-Jüttner distribution on a

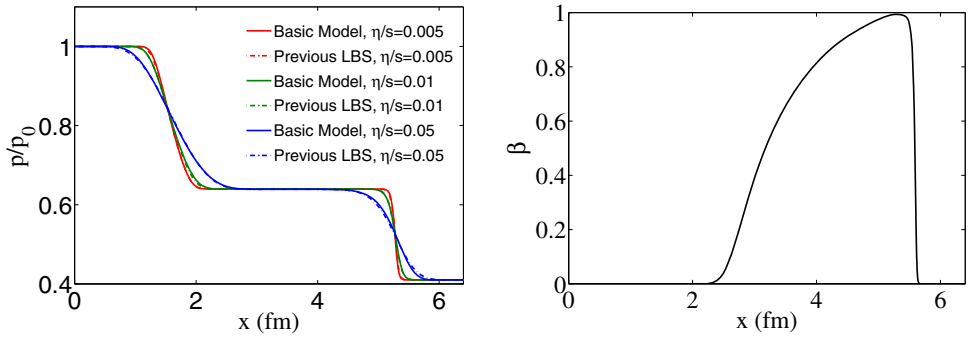

(a) (b)

Fig. 2. a) Comparison between the basic model and the previous LBS model at different η/s, for pressure profiles in the weakly relativistic regime ($\beta \sim 0.2$). b) Results of the simulation for the velocity profile in the ultra-high relativistic regime with $\eta/s = 0.01$ using the extended model.

set of orthogonal polynomials. To this end, we start by writing the Maxwell-Jüttner distribution in a simpler form, by introducing the following change of variables [20]: $\xi^\mu = (p^\mu/m)/c_s$, $\chi^\mu = U^\mu/c_s$, where $c_s = \sqrt{k_B T/m}$ and $W = c/c_s$. Therefore, we can write the Maxwell-Jüttner distribution as $f^{\text{eq}} = A\exp(-\xi_\mu \chi^\mu)$, and expand it using orthogonal polynomials of the following form:

$$f^{\text{eq}}(\boldsymbol{\xi}, \boldsymbol{x}, t) = w(\boldsymbol{\xi}) \sum_{n=0}^{\infty} \frac{a_{(n)}(\boldsymbol{x}, t)}{N_{(n)}} F_{(n)}(\boldsymbol{\xi}), \quad \text{with} \quad N_{(n)} = \int w F_{(n)} F_{(n)} \frac{d^3\xi}{\xi^0}, \tag{6}$$

where

$$a_{(n)}(\boldsymbol{x}, t) = \int f^{\text{eq}} F_{(n)} \frac{d^3\xi}{\xi^0}. \tag{7}$$

In order to construct the appropriate orthogonal polynomials, we introduce the corresponding weight function as the equilibrium distribution at the local rest frame, i.e., $w(\boldsymbol{\xi}) = A\exp(-W\xi^0)$, and compute the orthogonal polynomials using the Gram-Schmidt procedure. Employing the resulting polynomials, the coefficients $a_{(n)}$, $N_{(n)}$, and Eq. (6) we get the expansion of the Maxwell-Jüttner distribution.

The lattice configuration D3Q19 is used to discretize space. In order to find the discretized lattice weights, the following quadrature is applied:

$$\int R(\boldsymbol{\xi}) w(\boldsymbol{\xi}) \frac{d^3\xi}{\xi^0} = \sum_{i=1}^{N} R(\xi_i) w_i, \tag{8}$$

where $R(\boldsymbol{\xi})$ is an arbitrary polynomial of order $2N$, or less, which gives a system of linear algebraic equations to calculate the weights w_i. In the ultra-relativistic limit, the corresponding discretized model leads to the correct form of the energy-momentum tensor, with an ultra-relativistic equation of state, $\epsilon = 3p$.

In order to validate the accuracy of the model, the same numerical test for the shock wave in viscous quark-gluon plasma as in Sect. 2.1 is performed and the results are compared with the moment matching model (previous LBS) for different values of shear viscosity. The results reported in Fig. 2a show very good agreement. In fact, the proposed model can accurately resolve the shock wave in the Riemann problem in the range $\beta < 0.6$. At higher velocities, due to the compressibility effects

(high Mach numbers), the described numerical scheme shows spurious discontinuities in the velocity and pressure profiles, leading to numerical instabilities in the long-term evolution.

To overcome this problem, several extensions to the aforementioned scheme (basic model) are considered. 1) A modified version of the $D3Q19$ cell configuration is used, where the magnitude of the longer diagonal vectors is doubled. This cell configuration can support higher flow speeds since some of the discrete velocities go beyond first and second neighbors. 2) To discretize the spatial derivative in the streaming term of the Boltzmann equation a flux limiter scheme (min mod scheme) is utilized which efficiently diminishes the numerical instabilities in step discontinuities, e.g., in shock waves. 3) An additional term is added to the right hand side of the Boltzmann equation to include the bulk viscosity. Bulk viscosity plays an important role in highly compressible flows and enhances the numerical stability at high velocities. Indeed, the extended model is numerically robust even for very high velocities. Figure 2b shows the successful simulation of the Riemann problem in the ultra-relativistic regime when $\beta \sim 0.99$ and $\gamma(u) \sim 9$. For more details see Ref. [20].

2.3 Models with improved dissipation

In this section, we describe an improved RLB model, providing a more accurate description of dissipative phenomena in relativistic hydrodynamics than aforementioned RLB schemes. The procedure applies to the ultra-relativistic regime, in which the kinetic energy (temperature) far exceeds the rest mass energy. Although the models described in Sect. 2.1 and Sect. 2.2 show very good accuracy for low values of η/s, they are not able to reproduce the right velocity and pressure profiles for the Riemann problem in quark-gluon plasmas, for large values of η/s. This is because, in these models, the third order moment of the equilibrium distribution does not match its continuum counterpart. Here, we develop a new LB model capable of reproducing the third order moment of the continuum equilibrium distribution. The model is based on a single distribution function and satisfies conservation of both number of particles and momentum-energy equations, where the single relaxation time collision operator proposed by Anderson and Witting, Eq. (3), is used.

Hereafter, we will use natural units, $c = k_B = 1$, and work in the ultrarelativistic regime, $\xi \equiv mc^2/k_BT \ll 1$. Similar to what is described in Sect. 2.2 (but here for the ultra-relativistic limit where the rest mass energy is negligible), we calculate a basis of orthonormal polynomials in Cartesian coordinates using the equilibrium distribution at rest, $w(p^0) = f^{\mathrm{eq}}(\mathbf{u} = 0)$ as a weight function, where in the ultra-relativistic regime we have $p^0/T = \sqrt{\mathbf{p}^2/T^2 + m^2/T^2} \simeq p/T$, being $p = \sqrt{\mathbf{p}^2}$. Once the polynomials are obtained, they are used to perform the expansion of the complete equilibrium distribution f^{eq}.

In order to discretize the above moment projection of the equilibrium distribution, we must choose a set of discrete 4-momentum vectors that satisfies the orthonormality condition, namely

$$\int w(p^0) J_l(p^\mu) J_k(p^\mu) \frac{d^3p}{p^0} = \sum_i w_i J_l(p_i^\mu) J_k(p_i^\mu) = \delta_{lk}, \tag{9}$$

where J_k are the orthonormal polynomials. Note that the quadrature relation (as in Eq. 8) is used for the first equality. Indeed, in a cubic cell of length $\delta x = 1$ there are only 6 neighbors, which are not sufficient to satisfy the orthogonality conditions and the third order moment of the equilibrium distribution. However, we can multiply the Boltzmann equation by a constant R at both sides, and perform a time transformation

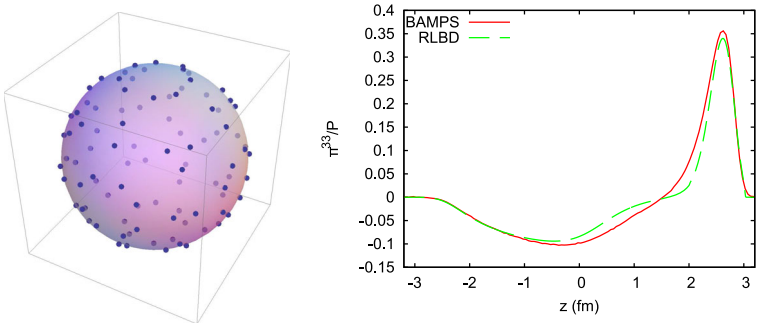

(a) (b)

Fig. 3. a) Directions of the velocity vectors ϑ_i for the third order model. The radius of the sphere is $R = \sqrt{41}$. The points represent lattice sites belonging to the sphere surface. b) One component of the viscous pressure tensor for shock waves in quark-gluon plasma, with $\eta/s = 0.1$. Here RLBD denotes the present third order model.

(dilatation), $\delta t \to R\delta t'$ and $\tau \to R\tau'$. Thus we can write the 4-momentum vectors $p^\mu = p^0(1, \vartheta/R)$, where we have defined $\vartheta = Rv^a$, v^a being the microscopic velocity. The radius of the sphere (R) should be chosen such that the lattice points that belong to the surface of the sphere and the cubic lattice exhibit enough symmetries to satisfy both aforementioned conditions. This can be done by imposing that R^2 must be a positive integer number, such that the microscopic velocity vectors satisfy $(v_i^x)^2 + (v_i^x)^2 + (v_i^z)^2 = R^2$. Thus, starting with $R = 1$ and increasing by one systematically, we calculate the set of velocity vectors that satisfies the previous relation, and use those vectors to solve the orthogonality condition, Eq. (9). We have found that $R = 3$ and $R = \sqrt{41}$ lead to the smallest set of velocity vectors that are sufficient to recover up to the second and third order moment of the Maxwell-Jüttner distribution, respectively. In Fig. 3a we report the configuration of the velocity vectors ϑ to achieve the third order moment of the distribution function.

For the single relaxation time lattice Bhatnagar-Gross-Krook (LBGK) kinetic equation, the transport coefficients using the third order model for the ultrarelativistic gas are, $\mu = 0$ for the bulk viscosity, $\eta = (2/3)p(\tau - \delta t/2)$ for the shear viscosity, and $\lambda = (4/5T)p(\tau - \delta t/2)$ for the thermal conductivity. Numerical simulations of the Riemann problem for a quark-gluon plasma show that, compared to the previous models, the current scheme (third order) is remarkably more accurate for high values of η/s particularly at moderately relativistic regimes ($\beta \sim 0.6$). Figure 3b shows the result for the component π^{33} of the viscous pressure tensor compared with the results of BAMPS, where a good agreement is observed. For more details see Ref. [21].

3 Applications

3.1 Quark-gluon plasma

Quark-gluon plasma (QGP), a collection of strongly interacting quarks and gluons, represents one of the most exciting new states of matter. During its lifetime, the QGP is accurately described by hydrodynamic models of nearly perfect fluids [22]. Therefore, shock waves have been theoretically predicted [23] and experimentally observed [24]. The existence of such shock waves is very important, as it provides direct information about the speed of sound, and therefore, about the equation of state (EoS). As mentioned, our RLB models can successfully simulate shock waves

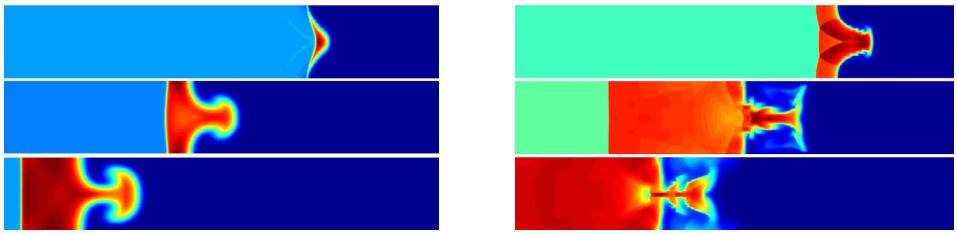

(a) Relativistic (b) Non-Relativistic

Fig. 4. Snapshots of the density field in the 2D shock tube Richtmyer-Meshkov instability for (a) relativistic case when $n_L/n_M = 28$ and $Ma_r = 2.4$ and (b) non-relativistic case when $n_L/n_M = 28$ and $Ma = 2.4$ at different times. For both cases, from the top to the bottom, snapshots corresponds to the times $t = 180$, $t = 720$, and $t = 1260$, respectively and blue to red denote low and high densities, respectively.

(Riemann problem) for a wide range of viscosities, at different velocities, i.e., low relativistic, mildly relativistic and highly relativistic regimes. See Figs. 1, 2 and 3b and Refs. [18,20,21] for more information.

3.2 Relativistic Richtmyer-Meshkov instability

As an application for the RLB method, here we study the relativistic effects on the Richtmyer-Meshkov (RM) instability. The Richtmyer-Meshkov instability is one of the fundamental fluid instabilities, which occurs whenever a shock wave passes through an interface, separating two fluids having different densities. The study of the RM instability is of great importance for understanding several phenomena ranging from high energy density physics [25] to astrophysics [26]. Considering the fact that, relativistic effects play a major role in many of these applications, studies of the relativistic RM instability contribute to the understanding of these phenomena.

Therefore, numerical simulations of RM instability in the linear and non-linear regimes for a wide range of density ratio and Mach number are performed. Here we are interested in a more generalised ideal gas equation of state given as $p = (\Gamma - 1)(\epsilon - n)$, where $\Gamma = c_p/c_v$ and c_p and c_v are specific heats at constant pressure and volume, respectively. Hence, some extensions to the RLB model for high velocities (proposed in Section 2.2) are required to deal with this equation of state. Firstly, for the collision operator, the model of Anderson-Witting (Eq. (3)) should be used which allows the coupling between the equations of conservation of energy-momentum and density four-flow. Secondly, the equilibrium distribution function needs to be modified by adding a term corresponds to non-negligible rest mass energy.

Moreover, we are also interested in finding a theoretical relation for the growth rate of the amplitude of the perturbation (v_f) in the linear regime of relativistic RM instability. Thus, we perform a linear stability analysis starting from the macroscopic conservation equations. The resulting growth rate has the form

$$v_f \equiv \frac{\partial h(t)}{\partial t} = \frac{(n_2 - n_1)kh_0 \triangle u}{\gamma(2p + \epsilon_2 + \epsilon_1)}. \tag{10}$$

Here $h(t)$ and k are the amplitude and wave number of the perturbation, respectively, h_0 is the initial amplitude, ϵ_1 (n_1) and ϵ_2 (n_2) are the energy densities (densities) at both sides of the interface, and p and $\triangle u$ are pressure and velocity jump at the interface, respectively. Note that this is a general expression which holds for any EoS,

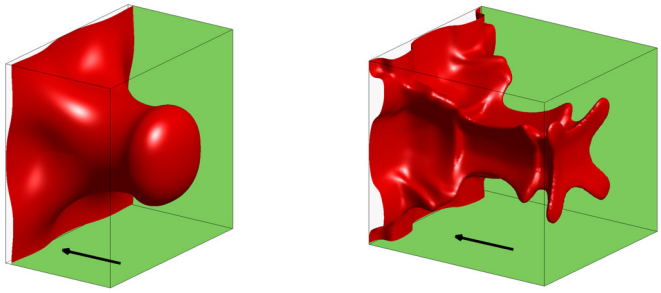

(a) Relativistic (b) Non-Relativistic

Fig. 5. Snapshots of the spikes in the 3D shock tube Richtmyer-Meshkov instability with square cross section when the pre-shock density ratio is 28 and the Mach number is 2.4 at time $t = 570$ for (a) relativistic and (b) non-relativistic cases. Arrows show the direction of the shock wave.

$\epsilon = \epsilon(T)$ and $p = p(T)$, where T is the temperature. One can immediately notice from Eq. (10) that relativistic effects decrease the amplitude growth rate compared to the non-relativistic RM instability. This is due to the Lorentz's factor γ as well as the contribution of the pressure to the inertia of the relativistic fluid (in the denominator). This increase in the inertia leads to a decrease of the amplitude growth rate of the instability, showing that relativistic effects tend to damp the instability.

Numerical simulations of shock tube RM instability are performed in 2D and 3D, where a shock wave traveling from right to left passes through a sinusoidal perturbation in the density. The single mode sinusoidal perturbation at the interface is considered. Hereafter the subscripts R, M, and L refer to the right hand side of the shock, the region between the shock and the initial perturbation, and the left hand side of the perturbation, respectively. The simulations have been performed for various pre-shock density ratios n_L/n_M and various values of the relativistic Mach number of the shock wave.

After passing the shock wave, both regions with different densities penetrate each other gradually, i.e., the lighter part creates bubbles and the heavier one forms spikes. This can be seen in Fig. 4a, which shows the results of the 2D simulation of the density field at different times after the shock wave passed through the initial perturbation. Finally, the spikes form the characteristic mushroom shape of the instability.

To demonstrate the relativistic effects and for the purpose of comparison, we have also performed a numerical simulation for the non-relativistic RM at the same density ratio and Mach number as in Fig. 4a. The results are presented in Fig. 4b which shows that, in the non-relativistic RM, the amplitude of the perturbation grows much faster at early times which leads to faster development and more complex structures of the instability at later times. This can also be seen in Fig. 5, where the results of the simulation for the 3D shock tube RM instability with square cross section is presented. In fact, this agrees with our prediction based on Eq. (10) where we argued that relativistic effects have damping effects on the instability.

3.3 Campylotic flows

All the RLB models described so far were developed for special relativity, where there is no intrinsic curvature in the space-time. Before discussing general relativity (see Sect. 4), we consider the case of flow in curved manifolds, in the non-relativistic context. Among all the applications for campylotic (curved) media [27], one can mention,

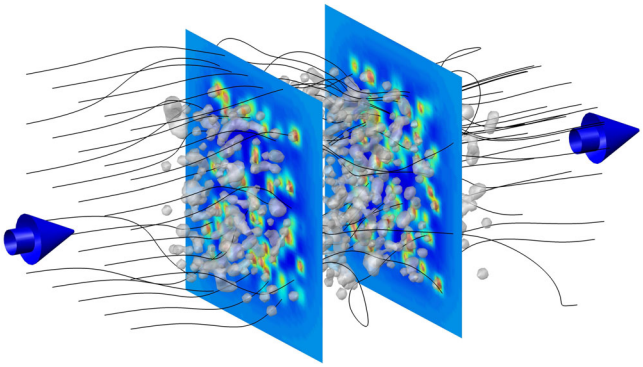

Fig. 6. Streamlines of a three-dimensional fluid moving through a campylotic medium. The colors denote the Ricci scalar R' (blue and red for low and high values, respectively). The gray bubbles isosurfaces stand at 1/5 of the maximum curvature of the system.

for instance, flow between two rotating cylinders and spheres, flow through porous media and solar photosphere [28]. Here, we present a new lattice kinetic scheme that can handle flows in virtually arbitrary complex manifolds in a very natural and elegant way, by resorting to a covariant formulation of the LB kinetic equation in general coordinates. The corresponding hydrodynamic equations in curved media are: $\partial_t \rho + (\rho u^\mu)_{;\mu} = 0$, and $\partial_t(\rho u^\mu) + T^{\mu\nu}_{;\nu} = 0$, where the notation $_{;\mu}$ denotes the covariant derivative with respect to spatial component μ, and ρ is the density and $T^{\mu\nu}$ is the energy tensor.

Since LB methods are based on kinetic theory, we construct our model by writing the Maxwell-Boltzmann distribution and the Boltzmann equation in general geometries. The former takes the form:

$$f^{\mathrm{eq}} = \frac{\rho}{(2\pi\theta)^{3/2}} \exp\left[-\frac{1}{2\theta} g_{\mu\nu}(\xi^\mu - u^\mu)(\xi^\nu - u^\nu)\right], \tag{11}$$

where θ is the normalized temperature, and ξ the microscopic velocity. The Boltzmann equation can be obtained from a more general expression, $df/dt = \mathcal{C}(f)$, where the total time derivative now includes a streaming term in velocity space due to external forces. Thus, we can write the Boltzmann equation as

$$\partial_t f + \xi^\mu \partial_\mu f - \Gamma^\mu_{\nu\gamma} \xi^\mu \xi^\gamma \partial_{\xi^\nu} f = \mathcal{C}(f). \tag{12}$$

Note that in our model the Christoffel symbols $\Gamma^i_{\gamma\nu}$ and metric tensor $g_{\mu\nu}$ are arbitrary and therefore we can model the fluid flow in curved spaces, whose metric tensor is very complicated and/or only known numerically. As usual, we implement an expansion of the Maxwell-Boltzmann distribution in Hermite polynomials, in order to recover the moments of the distribution up to third order in velocities to correctly reproduce the dissipation in the hydrodynamic equation. Note that the so-called standard lattices are not useful in the present context because of their low symmerty. Our scheme is based on higher-order D3Q41 lattice [29] and the discrete Boltzmann equation for our model takes the form,

$$f_i(x^\mu + c_i^\mu \delta t, t + \delta t) - f_i(x^\mu, t) = -\frac{\delta t}{\tau}(f_i(x^\mu, t) - f_i^{\mathrm{eq}}(x^\mu, t)) + \mathcal{F}_i \delta t, \tag{13}$$

where $\mathcal{F}_i$ is the forcing term, which contains the Christoffel symbols, and f_i^{eq} is the discrete form of the Maxwell-Boltzmann distribution. The method is validated

quantitatively for very simple campylotic media, by calculating the critical Reynolds number for the onset of the Taylor-Couette instability in concentric cylinders and spheres. Excellent agreement with analytical and experimental data is found [27].

By using the new numerical scheme, we simulate the flow through campylotic media consisting of randomly distributed spatial curvature perturbations (see Fig. 6). The flow is characterized by the number of curvature perturbations and the average Ricci scalar of the space. The campylotic media explored in this work are static, in the sense that the metric tensor and curvature are prescribed at the outset once and for all, and do not evolve self-consistently with the flow. For more information see Ref. [27].

4 General relativistic kinetic theory

The current versions of the relativistic LB do not deal yet with general relativistic flows. In this section, we present some prospects in the direction of developing a general relativistic lattice Boltzmann model.

We summarize the above results as follows: i) We constructed LB models for solving the energy-momentum equation of the dissipative relativistic fluid dynamics in flat time-space; that is, the focus was on giving a convenient LB formulation of the energy-momentum tensor equation. ii) A non-relativistic LB on a constant space-curved background (campylotic flow) was also constructed; In principle, this latter could be extended to solve the relativistic LB on a fixed gravitational background as well.

Now, general relativity requires a coupling between the energy-momentum tensor as the source term in the Einstein's equations (EE) for the metric tensor, i.e.

$$D_g f = -\omega(f - f^{eq}), \tag{14}$$

$$G_{\mu\nu} = T_{\mu\nu}, \tag{15}$$

where $G_{\mu\nu} = R_{\mu\nu} - \frac{1}{2}Rg_{\mu\nu}$ is the Einstein tensor and $T_{\mu\nu}$ is the matter tensor, including non-equilibrium matter fluctuations. In the above D_g stands for the covariant derivative in the metric $g_{\mu,\nu}$. The Boltzmann equation feeds the EE's with the matter tensor $T_{\mu\nu} = \int f p_\mu p_\nu dp$, while the EE's react back on the Boltzmann equation via the spacetime dependent metric field $g_{\mu\nu}(x^\lambda)$. In principle, there are two options to proceed with the numerical solution of the above Boltzmann-Einstein's equations.

The first is to consider the existing RLB framework, possibly generalizing it to take into account the metric tensor in the momentum-energy equation, and simultaneously solve the Einstein's equation by the most suitable method available in the numerical relativity literature. This is analogous to, say, the way one often does with thermal LB, where the temperature equation is solved separately by finite differences and only the momentum equation is left for LB.

A more radical alternative is to develop a separate kinetic equation for the metric tensor and solve it with LB techniques. It is clear that here we have "two-population" approach in mind, one population for energy-momentum, another one for the metric tensor. They are coupled in the sense that the equilibrium of the latter is informed by the energy-momentum from the former (to recover the EE's), whereas the metric tensor obtained as a moment of the second distribution is used as a forcing term in the first LB (as in campylotic case, for example). This decomposition can, in principle, profit from the recent consistent two-population picture developed in the context of thermal LB's [30] for a scalar field.

However, in general this task involves a number of genuinely new challenges, which will be briefly discussed in the subsequent section.

4.1 Kinetic formulation of the Einstein equations

To the best of our knowledge, no kinetic theory of spacetime has been formulated as yet; in fact whether such a theory exists altogether remains an open issue at the time of this writing. If such a theory did exist, one could proceed to develop a LB version by applying the polynomial projection techniques described earlier on in this paper. Nevertheless, a lattice kinetic solver for the Einstein equations (EE's) can be envisaged also in the absence of such a theory, somehow in the spirit of the moment-matching method described in the early part of this paper. Indeed, it is by now well-known that there exist many non-linear wave equations, besides Navier–Stokes equations, which can be formulated as kinetic equations in double-dimensional phase-space. These include the Korteveg-De Vries, Burgers and Gross-Pitaevskii equations and many others [31–34]. Since the EE's are also non-linear tensor wave equations, it is only natural to conjecture it should be possible to cast them in kinetic format too. To turn this idea into a concrete plan, however, a number of issues must be faced.

First, representation: the most appropriate hyperbolic representation of the EE's must be identified. This is a non-trivial task on its own, since it is known that the EE's can be formulated in many ways, depending on the choice of coordinates, dependent fields and ensuing constraints. Although equivalent in principle (and sometimes not even in principle!), these formulations might differ considerably in terms of their numerical implementations. In this respect, of special interest appears to be the harmonic coordinates representation, which has led to recent breakthroughs in the simulation of black hole mergers [35,36].

Second, tensorial disentanglement between non-linearity and non-locality: Once the appropriate representation is found, one should investigate whether it can be cast within the lattice kinetic stream-collide paradigm. At this point, it should be noted that in the Navier-Stokes equations, non-linearity and non-locality appear within the same term, $\mathbf{u}\nabla\mathbf{u}$: the fluid moves its own momentum along the trajectories defined by the momentum itself: a non-local quadratic self-coupling.

One of the key advantages of the kinetic stream-collide representation is that this confluence is disentangled, the non-linearity is conveyed to a local collision operator and the non-locality into a linear streaming operator. This is a major simplification, from both mathematical and computational viewpoints.

In the case of the EE's, the tangle between non-linearity and non-locality is significantly more involved. However, since the EE's non-linearities involve various combinations of the basic forms $g\Delta g$, $(\nabla g)^2$, where ∇ and Δ stand for tensorial generalizations of the Laplacian and gradient operators, there are good reasons to believe that disentanglement, although more elaborate, should still be possible. Incidentally, proving that this is possible would mark a major step towards the formulation of a kinetic theory of spacetime.

The above matter surely makes a very fascinating subject for future research, not only for computational purposes but also in terms of fundamental extensions of kinetic theory.

5 Conclusions

Several models of RLB have been reviewed in this study, which prove capable of simulating a broad range of relativistic hydrodynamic problems, from weakly-relativistic to fully-relativistic regimes and from nearly perfect (low viscosity) to high viscosity fluids. Shock waves in quark-gluon plasma, relativistic Richtmyer-Meshkov instability and curved manifolds are among the areas that are studied with these models. Extending the current models to include magnetohydrodynamics (MHD) [37] and general relativistic effects are objects of future research. Extensions of the current

formalism to the fully-coupled Boltzmann-Einstein's equations stands out as a very fascinating topic for future research.

We acknowledge financial support from the European Research Council (ERC) Advanced Grant No. 319968- FlowCCS and financial support of the Eidgenssische Technische Hochschule Zürich (ETHZ) under Grant No. 0611-1. I.K. gratefully acknowledges support by the European Research Council (ERC) Advanced Grand No. 291094-ELBM. One of the authors (SS) kindly acknowledges illuminating discussions with F. Pretorius and S. Tremaine.

References

1. H. Chen, S. Chen, W. Matthaeus, Phys. Rev. A **45**, 5339 (1992)
2. R. Benzi, S. Succi, M. Vergassola, Phys. Rep. **222**, 145 (1992)
3. S. Succi, *The lattice Boltzmann Equation for Fluid Dynamics and Beyond* (Oxford University Press, New York, 2001)
4. M. Mendoza, F. Wittel, H. Herrmann, Eur. Phys. J. E **32**, 339 (2010)
5. S. Succi, The Eur. Phys. J. B **64**, 471 (2008)
6. C.K. Aidun, J.R. Clausen, Annu. Rev. Fluid Mech. **42**, 439 (2010)
7. K. Novoselov, A. Geim, S. Morozov, D. Jiang, M. Katsnelson, I. Grigorieva, S. Dubonos, Nat. Lett. **438**, 197 (2005)
8. M. Müller, J. Schmalian, L. Fritz, Phys. Rev. Lett. **103**, 025301 (2009)
9. M. Mendoza, H. Herrmann, S. Succi, Sci. Rep. **3** (2013)
10. M. Mendoza, H. Herrmann, S. Succi, Phys. Rev. Lett. **106**, 156601 (2011)
11. E. Shuryak, Prog. Part. Nuc. Phys. **53**, 273 (2004)
12. P.K. Kovtun, D.T. Son, A.O. Starinets, Phys. Rev. Lett. **94**, 111601 (2005)
13. S. Siegler, H. Riffert, Astrophys. J. **531**, 1053 (2008)
14. M. Dubal, Comput. Phys. Commun. **64**, 221 (1991)
15. M. Mendoza, B. Boghosian, H. Herrmann, S. Succi, Phys. Rev. Lett. **105**, 014502 (2010)
16. C. Marle, C. Hebad, Seances Acad. Sci. **260**, 6539 (1965)
17. J. Anderson, H. Witting, Physica **74**, 466 (1974)
18. M. Mendoza, B.M. Boghosian, H.J. Herrmann, S. Succi, Phys. Rev. D **82**(10), 105008 (2010)
19. I. Bouras, E. Molnar, H. Niemi, Z. Xu, A. El, O. Fochler, C. Greiner, D.H. Rischke, Phys. Rev. Lett. **103**, 032301 (2009)
20. F. Mohseni, M. Mendoza, S. Succi, H.J. Herrmann, Phys. Rev. D **87**, 083003 (2013)
21. M. Mendoza, I. Karlin, S. Succi, H. Herrmann, Phys. Rev. D **87**, 065027 (2013)
22. Z. Xu, C. Greiner, H. Stöcker, Phys. Rev. Lett. **101**, 082302 (2008)
23. W. Scheid, H. Müller, W. Greiner, Phys. Rev. Lett. **32**, 741 (1974)
24. H.H. Gutbrod, K.H. Kampert, B. Kolb, A.M. Poskanzer, H.G. Ritter, R. Schicker, H.R. Schmidt, Phys. Rev. C **42**, 640 (1990)
25. V. Goncharov, Phys. Rev. Lett. **82**, 2091 (1999)
26. D. Arnett, Astrophys. J. Supp. Ser. **127**, 213 (2000)
27. M. Mendoza, S. Succi, H. Herrmann, Sci. Rep. **3** (2013)
28. E. Priest, *Solar Magneto-hydrodynamics*, Geophysics and astrophysics monographs (D. Reidel Pub. Co., 1984), ISBN: 9789027718334
29. S.S. Chikatamarla, I.V. Karlin, Phys. Rev. E **79**, 046701 (2009)
30. I. Karlin, D. Sichau, S. Chikatamarla, Phys. Rev. E **88**, 063310 (2013)
31. G. Yan, J. Zhang, Math. Comput. Simulat. **79**, 1554 (2009)
32. J. Zhang, G. Yan, Physica A **387**, 4771 (2008)
33. S. Palpacelli, S. Succi, R. Spigler, Phys. Rev. E **76**, 036712 (2007)
34. S. Palpacelli, S. Succi, Phys. Rev. E **77**, 066708 (2008)
35. F. Pretorius, W. Israel, Classical Quant. Grav. **15**, 2289 (1998)
36. F. Pretorius, Phys. Rev. Lett. **95**, 121101 (2005)
37. M. Ottaviani, F. Romanelli, R. Benzi, M. Briscolini, P. Santangelo, S. Succi, Phys. Fluids B **2**, 67 (1990)